

Aggregate and Firm-Level Stock Returns During Pandemics, in Real Time*

Laura Alfaro[†] Anusha Chari[‡] Andrew Greenland[§] Peter K. Schott[¶]

May 5, 2020

Preliminary and Incomplete
Comments Welcome!

Most recent version is [here](#)

First Draft: March 25, 2020

Abstract

We link unexpected changes in the trajectory of pandemics to aggregate and firm-level stock returns during COVID-19 and SARS. We find that an unanticipated doubling of *predicted* infections forecasts next-day declines in aggregate market value of 4 to 11 percent. Exploiting the same variation, we show that COVID-19-related losses in market value vary widely across US firms, and rise with their capital intensity and leverage. Consequently, US states whose employment is concentrated in labor-intensive firms exhibit milder declines in average market value. They also have higher increases in initial jobless claims per worker, suggesting investors value precisely what workers loathe – the relative ease with which labor versus capital costs can be shed as revenues decline.

*This paper is preliminary and incomplete. Missing citations and discussions of related research will be added in future drafts. We thank Nick Barberis, Lorenzo Caliendo, Teresa Fort, Mihai Ion, Ed Kaplan, John Lopresti, and Duke and UNC TEAM seminar participants at for comments and suggestions. We thank Alex Schott and Mengru Wang for excellent research assistance.

[†]Harvard Business School & NBER (lalfaro@hbs.edu).

[‡]UNC Chapel Hill & NBER (achari@unc.edu).

[§]Martha and Spencer Love School of Business, Elon University (agreenland@elon.edu).

[¶]Yale School of Management & NBER (peter.schott@yale.edu).

1 Introduction

The tension between Wall-Street and Main Street during the COVID-19 pandemic is palpable. In the early weeks of the outbreak, US equity markets dropped 35 percent. Then, even as reported infections continued to rise, and jobless claims surged, the stock market rallied. In this paper we investigate how information about the expected impact of pandemics is incorporated into aggregate and firm-level stock returns, *day by day*. Our results provide a rationale for the seemingly divergent paths of the equity and labor markets.

We begin by showing that unanticipated changes in *predicted* infections based on daily re-estimation of simple epidemiological models of infectious disease forecast next-day stock returns. While our focus is on the current COVID-19 crisis in the United States, we find a similar pattern during the 2003 SARS outbreak in Hong Kong. In both cases, larger changes in model predictions are associated with greater changes in market returns, in both directions.¹ Estimates for the United States thus far indicate that a doubling (halving) of predicted COVID-19 infections is associated with a decline (increase) of 4 to 10 percent in the Wilshire 5000 index. These findings are consistent with investors using such models to update their beliefs about the economic consequences of the outbreak as the disease progresses, in real time. They also suggest that equity markets may recover, and become less responsive to new cases, as the trajectory of the pandemic becomes more certain. As a consequence, they provide an explanation for the confusion expressed in recent newspaper articles about the recovery of the US stock market in April: this recovery coincides with a flattening out of unanticipated changes in predicted infections.²

We also examine exposure to COVID-19 at the industry and firm levels. We show that industries which might promote infection – Accommodations, Entertainment and Transportation – exhibit the greatest exposure to the pandemic, and the largest declines in market value. Education, Professional Services and Finance, by contrast, are less sensitive, likely due to a greater ability to continue operations online. At the firm level, we find that COVID-19-driven changes in market value are almost universally negative, that they vary widely both within and across sectors, and that more capital-intensive, more debt-laden, and less profitable firms exhibit larger declines.³

We interpret these results as signaling investors' expectation that firms which are more able to shed costs during the pandemic will have smaller losses, and thus relatively higher returns.⁴ As debt is non-dischargeable, and nearly all property, plant and equipment is sunk in a macroeconomic downturn of COVID-19's magnitude, debt-laden and capital-intensive firms are less likely to be able to reduce costs as revenues decline. Labor-intensive firms' relatively high returns, by contrast, anticipate the relative ease with which workers (versus capital) can be furloughed or dismissed as the economy contracts.

Further evidence in favor of this mechanism comes from analysis of job loss across regions. We construct county and state measures of exposure to COVID-19 as the employment weighted average changes in market value of the 4-digit NAICS sectors they produce (Bartik, 1991). Intuitively, given the firm results just summarized, we find that states with a greater proportion of labor-intensive companies exhibit less decline in average market value. Using a difference-in-differences specification, we demonstrate that these states also experience *greater* growth in initial jobless

¹We are expanding the set of countries we analyze for the COVID-19 outbreak, and are investigating other pandemics, e.g., the 2009 H1N1 outbreak. These results will appear in a future draft.

²See, for example, "Prescient or Pollyannaish? Explaining the Market's Rally" in the April 18, 2020 edition of the *Wall Street Journal*.

³Ramelli and Wagner (2020) and Albuquerque et al. (2020) also document the negative association between market returns and debt during COVID-19.

⁴Baker et al. (2020) show that a near ubiquitous decline in US consumption during late March and April.

claims per worker after the onset of COVID-19 versus before. We believe the interpretation of this initially counter-intuitive result is that labor-intensive firms both have more workers to let go, and are more likely to do so to cut costs. To the best of our knowledge, we are the first to use equity prices to quantify the spatial incidence of a macroeconomic shock, and among the first to examine regional variation in COVID-19-driven initial jobless claims.

Our analysis contributes to several literatures. First, we add to the very large body of research on asset pricing that examines the predictability of stock returns (e.g. [Campbell and Shiller \(1988\)](#), [Fama and French \(1988\)](#)) and, more specifically, to recent research examining the financial market consequences of COVID-19, lead by [Ramelli and Wagner \(2020\)](#). One set of papers in this burgeoning literature associates abnormal returns during the pandemic in the spirit of [Ball and Brown \(1968\)](#) and [Fama et al. \(1969\)](#) to various firm characteristics.⁵ A second set of papers seeks to identify channels of firm exposure via ex-ante observable firm or aggregate characteristics.⁶

While similar in spirit, our analysis differs from these two sets of papers both methodologically and quantitatively, as we relate returns to exogenous changes in investors' information about the trajectory of the pandemic, as it unfolds. Specifically, we model cumulative infections during an outbreak as following either an exponential or a logistic curve. We re-estimate the parameters of these models each day of the outbreak using information on reported cases up to that day. More precisely, we predict infections for trading day t using the cumulative counts as of the end of days $t - 1$ and $t - 2$. The differences in these forecasts represent *unanticipated* changes in the trajectory of the disease due to newly available information, and we examine how they covary with both aggregate and firm-level market returns on day t .⁷

As a robustness exercise, we demonstrate that the information in daily *predicted* infections dominates the most recent change in *reported* infections in forecasting stock returns. This dominance is understandable, in that the anticipated portion of the most recent reported case growth has already been priced into equities. It is precisely the *unanticipated* portion of this growth, however, that updates investors' expectations regarding the eventual number of infections, and the speed with which that number may be reached. This unanticipated information relates directly to economic consequences, as a jump in estimated share of the population that ultimately will be infected suggests a larger labor supply shock, while an increase in the estimated growth rate of infections has implications for healthcare capacity constraints. We also show that our results for the United States are robust to the inclusion of coarse controls for changes in federal and local policy.

Relative to existing research on the financial implications of COVID-19, our approach offers three benefits. First, it does not require us to calculate firms' expected normal rate of return with the aid of an asset pricing model such as the CAPM ([Sharpe, 1964a](#)) during a period before COVID-19. Indeed, estimates of abnormal returns utilizing such models may be mis-specified if their true values can be inferred only in the presence of disaster risk ([Bai et al., 2019](#)). Second, our approach yields firm-level measures of exposure without identifying their channels ex-ante, and without attributing all aggregate movement in returns to COVID-19. Given the unprecedented nature of this event, this benefit is sizeable. Finally, by exploiting changes in the forecasted trajectory of the pandemic between market close on day $t - 1$ and opening on day t , our approach exploits only new information about the trajectory of the pandemic and therefore can rationalize both market

⁵See, for example, [Ramelli and Wagner \(2020\)](#); [Albuquerque et al. \(2020\)](#); [Ru et al. \(2020\)](#).

⁶See, for example, [Baker et al. \(2020\)](#); [Fahlenbrach et al. \(2020\)](#); [Ding et al. \(2020\)](#); ?

⁷We emphasize that we are *not* epidemiologists and are *not* outlining a method to characterize the true path of pandemics. Nor are we, like [Piguillem and Shi \(2020\)](#) and [Berger et al. \(2020\)](#), trying to infer the efficacy of various intervention strategies. Such efforts, while of immense value, require data which may not be available until after the outbreak is substantially underway. Rather, we view real-time changes in the predicted severity of an outbreak as potentially useful summary statistics of its ultimate economic consequences.

upsangs and downturns. Our findings suggest that investors, facing substantial uncertainty about the true economic fallout of this realized tail risk (Knight, 1921; Keynes, 1937), may be availng themselves of changes in daily case forecasts as a summary statistic for the ultimate scale and economic fallout of the epidemic.

Our paper also contributes to the very large literature in public health which attempts to explain the trajectory of infections during a pandemic.⁸ In contrast to that research, we link changes in the estimated parameters and predictions of these models in real time to economic outcomes. To reiterate, we do not claim that the evolution of a pandemic must follow a purely exponential or logistic growth path. Rather, we explore whether the predictions of these models are informative of economic conditions, as manifest in their correlation with the market.⁹

Finally, this paper relates to a rapidly emerging literature studying the aggregate economic consequences of COVID-19, and a more established literature investigating earlier pandemics. Barro et al. (2020) draws parallels between COVID-19 and the “Spanish Flu” to forecast changes in economic activity, while Baker et al. (2020) documents that the COVID-19 pandemic is the first infectious disease outbreak whose mention in the press is associated with a large daily market movement. Our analysis complements the equity market studies of Gormsen and Kojien (2020) and Baker et al. (2020), who link COVID-19 financial market reactions to future GDP growth. It also relates to the labor market studies of Cajner et al. (2020) and Coibion et al. (2020), which analyze employment trends during COVID-19, and the examinations of labor market interactions during COVID-19 more directly in Humphries et al. (2020) and Bartik et al. (2020). In contrast to these efforts, we exploit exogenous variation in investor’s expectations about the pandemic’s trajectory to identify aggregate and firm-level exposure, which we then link to labor market outcomes.

This paper proceeds as follows. Section 2 provides a brief description of infectious disease models and how investors might link the predictions of these models and to asset prices. Sections 3 and 4 apply our framework to COVID-19 and SARS. Section 5 concludes.

2 Modeling

In this section we outline how infectious disease outbreaks can be modeled in real time, and how investors might make use of the model’s estimated parameters.

2.1 Simple Models of Infectious Diseases

Exponential and logistic growth models are frequently used in biology and epidemiology to model infection and mortality. An exponential model,

$$C_t = ae^{(rt)} \tag{1}$$

predicts the cumulative number of cases on day t , C_t , as a function of the growth rate of infections in that country, r , the initial number of infected persons a , and time. In an exponential model, the number of infections per day continues to climb indefinitely. While clearly unrealistic ex-post, the exponential growth model is consistent with early stage pandemic growth rates.

In a logistic model (Richards, 1959), by contrast, the growth in infections grows exponentially initially, but then declines as the stock of infections approaches the population’s “carrying-capacity,”

⁸Early contributions to this literature include Ross (1911), Kermack and McKendrick (1927), Kermack and McKendrick (1937) and Richards (1959).

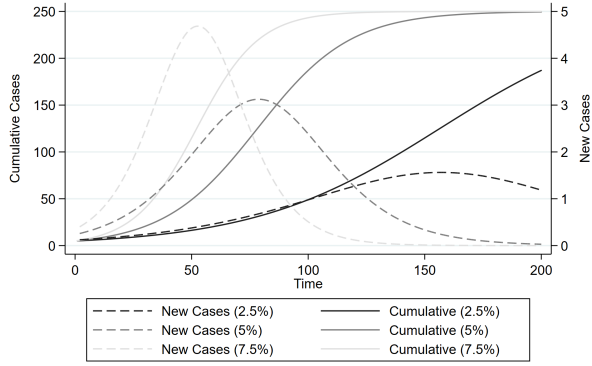
⁹For an interesting discussion on the complexities associated with modeling an outbreak in real time, see <https://fivethirtyeight.com/features/why-its-so-freaking-hard-to-make-a-good-covid-19-model/>.

i.e., the cumulative number of people that ultimately will be infected. Carrying capacity is generally less than the full population. The cumulative number of infections on day t is given by

$$C_t = \frac{k}{1 + ce^{(-rt)}}, \quad (2)$$

where k is the carrying, c is a shift parameter (characterizing the number of initially infected persons) and r is the growth rate. Figure 1 provides an example of logistic infections for three different growth rates (2.5, 5 and 7.5 percent) assuming $k = 250$ and $c = 50$. For each growth rate, we plot both the number of new cases each day (right axis) and the cumulative number of cases up to each day (left axis). As indicated in the figure, higher growth rates both shorten the time required to reach carrying capacity and increase the peak number of infections.

Figure 1: New and Cumulative New Cases Under the Logistic Model



Source: Authors' calculations. Figure compares new and cumulative infections from days 1 to 200 assuming a logistic model with $k = 250$ and $c = 50$ and noted growth rates (r).

Given data on the actual evolution of infections, the two parameters in equation 1 and the three parameters in equation 2 can be updated each day using the sequence of infections up to that date. We estimate these sequences using STATA's nonlinear least squares command (nl).¹⁰ This command requires a vector of starting values, one for each parameter to be estimated.

We encounter two problems during our estimation of logistic functions in our applications below. First, estimates for each day t are sensitive to the choice of starting values for that day, particularly in the initial days of the pandemic. This feature of the estimation is not surprising: when the number of cases is relatively small, a wide range of logistic curves may be consistent with the data, and the objective function across them may be relatively flat.

To increase the likelihood that our parameter estimates represent the *global* solution, we estimate 500 epidemiological models for each day, 250 for the logistic case, and 250 for the exponential case. In each iteration we use a different vector of starting values. For each day t , our first starting values are the estimated coefficients from the prior day, if available.¹¹ In the case of the logistic model, we then conduct a grid search defined by all triples $\{r, c, k\}$ such that

$$\begin{aligned} r &\in \{0.01, 0.21, 0.41, 0.61, 0.81\} \\ c &\in \{\widehat{c^{t-1}}, 2 * \widehat{c^{t-1}}, 4 * \widehat{c^{t-1}}, \dots, 10 * \widehat{c^{t-1}}\} \end{aligned}$$

¹⁰We are exploring other estimation procedures for use in a future draft, including use of SIR and SEIR models, e.g., Li et al. (2020) and Atkeson (2020).

¹¹If the prior day did not converge, we use the most recent prior day for which we have estimates.

$$k \in \{\widehat{k^{t-1}}, 2 * \widehat{k^{t-1}}, 3 * \widehat{k^{t-1}}, \dots, 10 * \widehat{k^{t-1}}\}$$

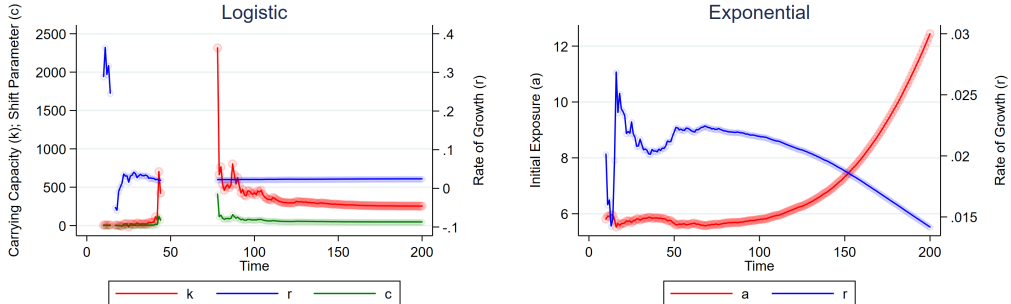
where hats over variables indicate prior estimates, and superscripts indicate the day on which they are estimated. If more than one of these initial starting values produces estimates, we choose the parameters from the model with the highest adjusted R^2 . We estimate the exponential model similarly.

The second, more interesting, problem that we encounter during estimation of the logistic outbreak curves is that STATA's `n1` routine may fail to converge. This failure generally occurs in the transition from relatively slow initial growth to subsequent, more obviously exponential growth as the pandemic proceeds. During this phase of the outbreak, the growth in the number of new cases each day is too large to fit a logistic function, i.e., the drop in the growth of new cases necessary to estimate a carrying capacity has not yet occurred.¹²

In our application below, we re-estimate both exponential and logistic parameters each day of an outbreak. To fix ideas, we simulate a 200-day cumulative logistic disease outbreak by generating a sequence of $C_t = \frac{k}{1+ce^{-rt}} + |\epsilon_t|$ for $t \in (1 : 200)$, assuming $k = 250$, $r = .025$, $c = 50$ and $|\epsilon_t|$ is the absolute value of a draw from a standard normal distribution. For each day t , we estimate logistic and exponential parameters using the sequence of simulated infections up to that day.

Figure 2 displays the results. Both sets of parameter estimates are volatile in the early stage of the outbreak. Logistic parameters are not available from days 47 through 78 due to lack of convergence, but settle down shortly thereafter, as the data increasingly conform to underlying logistic path. Exponential parameters are available for each day, but do not settle down as time goes on. The intuition for the unending increase in \widehat{a}_t and decline in \widehat{r}_t is as follows: because the simulated data are logistic, the only way to reconcile them with an exponential function is to have the estimate of initial exposure (\widehat{a}_t) rise as the estimate of the growth rate, \widehat{r}_t , drops.

Figure 2: Parameter Estimates Using Simulated Logistic Pandemic



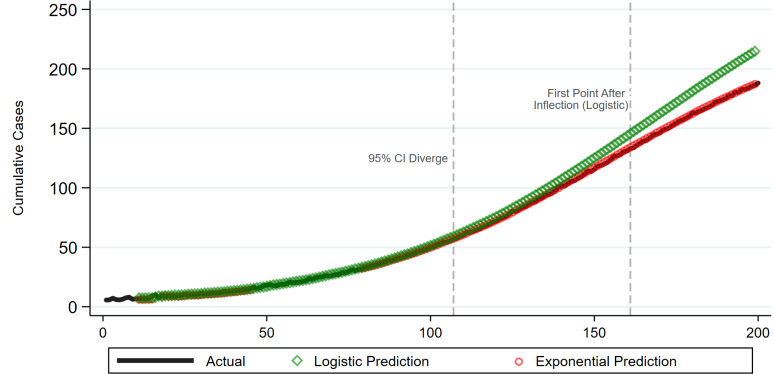
Source: authors' calculations. The left panel plots the sequence of logistic parameters, \widehat{k}_t , \widehat{c}_t and \widehat{r}_t , estimated using the information up to each day t on simulated data (see text). Right panel of Figure plots the analogous sequence of exponential parameters, \widehat{a}_t and \widehat{r}_t , using the same data. Missing estimates indicate lack of convergence (see text). Circles represent estimates. Solid lines connect estimates.

Figure 3 compares predicted cumulative cases for each model for each day t using the parameter estimates from day $t - 1$. We denote these predictions \widehat{C}_t^{t-1} , where the superscript $t - 1$ refers to the timing of the information used to make the prediction, and the subscript refers to the day being predicted. As illustrated in the figure, predictions for the two models line up reasonably well during the initial phase of the pandemic. Their 95 percent confidence intervals (not shown) cease overlapping on $t = 104$. After this point, the exponential model continues to project an

¹²In a future draft we will consider an estimation strategy that nests these functions.

ever-increasing number of infections, while the logistic model’s predictions head towards the “true” carrying capacity of 250.

Figure 3: Simulated Pandemic Daily Predictions (\widehat{C}_t^{t-1})



Source: authors’ calculations. Figure compares simulated “actual” cumulative infections to predicted infections (\widehat{C}_t^{t-1}) under the logistic and exponential models. The prediction for each day t is based on the information available up to day $t - 1$. The two vertical lines in the figure note when the 95 percent confidence intervals of the two models’ predictions (not shown) initially diverge, and when the logistic model’s estimates first indicate that its inflection point has passed.

2.2 Modeling Economic Impact

Predicted cumulative cases for day t based on day $t - 1$ information, \widehat{C}_t^{t-1} , can be compared to the day t forecast made with day $t - 2$ information, \widehat{C}_t^{t-2} . The log difference in these predictions,

$$\Delta \ln \left(\widehat{C}_t^{-2,-1} \right) = \ln \left(\widehat{C}_t^{t-1} \right) - \ln \left(\widehat{C}_t^{t-2} \right), \quad (3)$$

captures *unexpected* changes in severity of the outbreak between these two days.¹³ This potentially noisy “news” may be an important input into investors’ assessment of the economic impact of a pandemic. For example, a jump in estimated carrying capacity suggests a larger ultimate supply shock in terms of lost labor supply, while an uptick in the estimated growth rate has implications for healthcare capacity constraints.¹⁴

3 Application to COVID-19

In this section we provide real-time estimates of the outbreak parameters and infection predictions for COVID-19 in the United States. We then examine the relationship between changes in these predictions and both aggregate and firm-level returns in the United States.

¹³Timing is as follows. The number of infections on day $t - 1$ is observed after the market closes on that day but before the market opens on day t . This day $t - 1$ information is used to predict the number of cases for day t , \widehat{C}_t^{t-1} , which is compared to \widehat{C}_t^{t-2} .

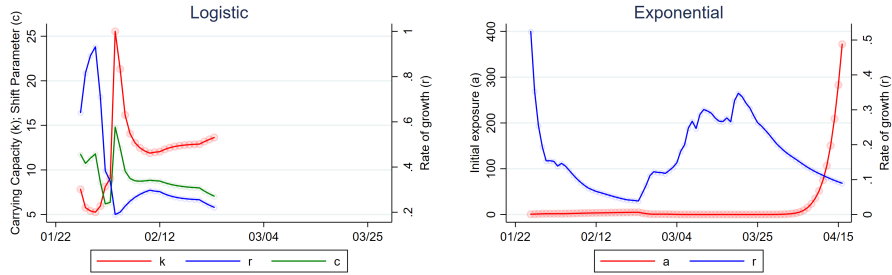
¹⁴As noted in the introduction, the evolution of these parameters may also trigger policy “events” either directly or as a result of their economic consequences, which may alter the underlying parameters of the outbreak. We do not currently account for such feedback, but plan to do so in a future draft.

3.1 Epidemiological Model Parameters

Data on the cumulative number of COVID-19 cases in the United States as of each day are from the Johns Hopkins Coronavirus Resource Center.¹⁵ The first COVID-19 case appeared in China in November of 2019, while the first cases in the United States and Italy appeared on January 20, 2020. Our analysis begins on January 22, 2020, the first day that the World Health Organization began issuing situation reports detailing new case emergence internationally. Appendix Figure A.1 displays the cumulative reported infections in the United States from January 22 through April 10, 2020.

We estimate logistic and exponential parameters (equations 1 and 2) for the United States by day as discussed in Section 2.1. The daily parameter estimates for the logistic estimation, \hat{k}_t , \hat{c}_t and \hat{r}_t are displayed the left panel of Figure 4, while those for the exponential model, \hat{a}_t and \hat{r}_t , are reported in the right panel. Gaps in the time series in either figure represent lack of convergence.

Figure 4: Parameter Estimates for COVID-19



Source: Johns Hopkins Coronavirus Resource Center and authors' calculations. The left panel plots the sequence of logistic parameters, \hat{k}_{it} , \hat{c}_{it} and \hat{r}_{it} , estimated using the cumulative infections in the US up to each day t . Right panel plots the analogous sequence of exponential parameters, \hat{a}_{it} and \hat{r}_{it} , using the same data. Missing estimates indicate lack of convergence (see text). Circles represent estimates. Solid lines connect estimates. Data currently extend to Friday March 27, 2020.

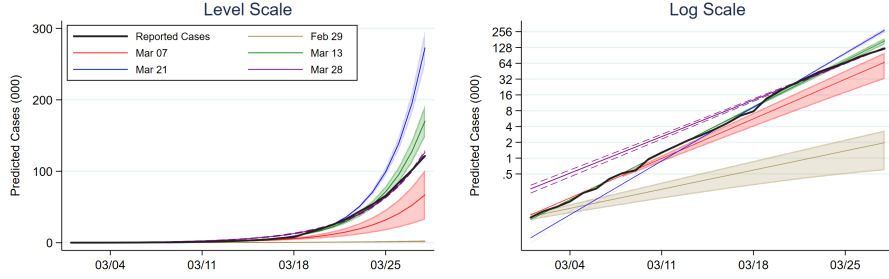
Logistic parameter estimates for the United States fail to converge after February 23, when the number of cases jumps abruptly from 15 to 51. That no parameter estimates are available after this date suggests that growth in new cases observed thus far is inconsistent with a leveling off, or carrying capacity, at least according to our estimation method. The exponential model, by contrast, converges for all days. As a result, we focus on the exponential model for the remainder of our analysis.

As the sharp changes in US exponential model parameters suggest, predicted cumulative infections vary substantially depending upon the day in which the underlying parameters are estimated. Figure 5 highlights this variability by comparing predicted cumulative infections based on the information available as of February 29 and March 7, 13, 21 and 28. The left panel displays these projections in levels, while the right panel uses a log scale. The five colored lines in the figure trace out each set of predictions. Dashed lines highlight 95 percent confidence intervals around these predictions. Finally, the confidence intervals are shaded for all days following the day upon which the prediction is based. To promote readability, we restrict the figure to the period after February 29. The black, solid line in the figure represents actual reported cases.

Predicted cumulative infections based on information as of February 29 are strikingly lower than predictions based on information as of March 21 due to the jump in reported cases between

¹⁵These data can be downloaded from <https://github.com/CSSEGISandData/COVID-19> and visualized at <https://coronavirus.jhu.edu/map.html>.

Figure 5: Predicted Cumulative Cases Using Different Days' Estimates (COVID-19)

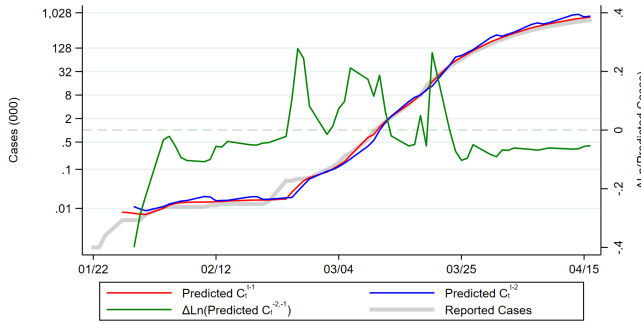


Source: Johns Hopkins Coronavirus Resource Center and authors' calculations. Figure displays predicted cases for the United States from March 18 onwards using the cumulative reported cases as of five dates: February 29, March 7, March 13, March 21 and March 28. Dashed lines represent 95 percent confidence intervals. Confidence intervals are shaded for all days after the information upon which the predictions are based.

those days. Indeed, according to the parameter estimates from March 21, US cases would number close to 300 thousand by the end of March. Equally striking is the downward shift in predicted cumulative cases that occurs between March 21 and March 28. It is precisely these kinds of changes in predicted cumulative cases that our analysis seeks to exploit.

Figure 6 uses the exponential parameter estimates in Figure 4 to plot \widehat{C}_t^{t-1} and \widehat{C}_t^{t-2} , i.e., the predicted number of cases on day t using the information up to day $t-1$ and day $t-2$. Magnitudes for these cumulative cases are reported on the left axis.

Figure 6: Daily Logistic Predictions (\widehat{C}_t^{t-1} and $\Delta \ln(\widehat{C}_t^{t-2, -1})$) for COVID-19



Source: Source: Johns Hopkins Coronavirus Resource Center and authors' calculations. Left axis reports the predicted cumulative cases for day t using information as of day $t-1$, \widehat{C}_t^{t-1} , and day $t-2$, \widehat{C}_t^{t-2} , under the exponential model. Right axis reports the log change in these two predictions, $\Delta \ln(\widehat{C}_t^{t-2, -1})$. Data currently extend to Friday April 10, 2020.

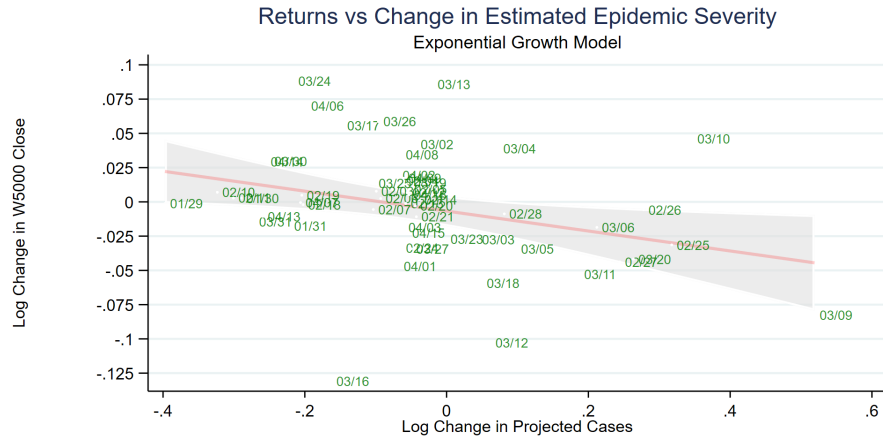
The right axis in Figure 6 reports $\Delta(\widehat{C}_t^{t-2, -1})$, the log difference in these two predictions. Intuitively, \widehat{C}_t^{t-1} and \widehat{C}_t^{t-2} for the most part track each other closely. The former rises above the latter on days when reported cases jump, while the reverse happens when new cases are relatively flat. The scalloped pattern of exhibited by \widehat{C}_t^{t-2} after March 25 captures the relatively smooth decline in \widehat{a}_{it} and rise in \widehat{r}_{it} (displayed in Figure 4) required for the exponential function to capture the increasingly logistic data.

3.2 Aggregate US Returns During COVID-19

We examine the link between changes in model predictions and aggregate US stock via the Wilshire 5000 index.¹⁶ We choose this index for its breadth, but note that results are qualitatively similar for other US market indexes.

Figure 7 plots the daily log change in the Wilshire 5000 index against unanticipated increases in cases, $\widehat{\Delta \ln(C_t^{-2,-1})}$. Their negative relationship indicates that returns are higher when the difference in predictions is lower, and *vice versa*. In particular, the approximate 20 percent decline in predicted cases that occurs on March 24 coincides with a greater than 9 percent growth in the market index.

Figure 7: Change in Predicted COVID-19 Cases ($\widehat{\Delta C_t^{-2,-1}}$) vs Aggregate Market Returns



Source: Johns Hopkins Coronavirus Resource Center, Yahoo Finance and authors' calculations. Figure displays the daily log change in the Wilshire 5000 index against the log change in predicted cases under the exponential model for day t based on day $t-1$ and day $t-2$ information. Sample period is January 22 to April 10, 2020.

We compare aggregate equity returns on day t to the difference in forecasts for that day formally using an OLS regression,

$$\Delta \ln(\text{Index}_t) = \alpha + \gamma_1 * \widehat{\Delta \ln(C_t^{-2,-1})} + \gamma_2 X_t + \epsilon_t. \quad (4)$$

where $\Delta \ln(\text{Index}_t)$ is the daily log change in either opening-to-opening or closing-to-closing prices in the Wilshire 5000, and X_t represents a vector of controls, e.g., changes in policy.¹⁷ The estimation period consists of 52 trading days from January 22 to April 10.¹⁸ The unit of observation is one day.

Coefficient estimates as well as robust standard errors are reported in Tables 1 and 2, where the former focuses on the daily opening-to-opening return and the latter on the daily closing-to-closing return. Coefficient estimates in the first column of each table indicate that a doubling of predicted cases using information from day $t-1$ versus day $t-2$ leads to average declines of -7.0 and -3.8

¹⁶Data for the Wilshire 5000 are downloaded from Yahoo Finance.

¹⁷We are currently exploring more flexible specifications, e.g., those which might capture the switch between exponential and logistic models, as well as those which reveal any over- or undershooting of reactions.

¹⁸The actual number of trading days between these two dates is 50. We lose 3 days due to lack of estimates in the initial days of the outbreak.

Table 1: Changes in Predicted COVID-19 Cases ($\widehat{\Delta C_t^{-1,-2}}$) vs Market Open Returns

	(1) $\Delta \ln(\text{Open})$	(2) $\Delta \ln(\text{Open})$	(3) $\Delta \ln(\text{Open})$	(4) $\Delta \ln(\text{Open})$	(5) $\Delta \ln(\text{Open})$	(6) $\Delta \ln(\text{Open})$
$\Delta \ln(C_t^{-2,-1})$	-0.040*** (0.013)	-0.049** (0.024)	-0.061** (0.024)	-0.063** (0.025)	-0.085** (0.033)	-0.055** (0.025)
$\Delta \ln(C_t^{-2,-1})$			0.019 (0.028)	0.026 (0.026)	0.028 (0.026)	0.006 (0.033)
$I(\Delta SIndex)$				-0.014 (0.014)		
$\Delta \ln(SIndex)$					-0.055 (0.061)	
Fiscal Stimulus						0.017 (0.013)
Constant	-0.007* (0.004)	-0.005 (0.004)	-0.008** (0.004)	-0.007* (0.004)	-0.006 (0.004)	-0.008* (0.004)
Observations	47	47	47	47	43	47
R^2	0.084	0.069	0.078	0.121	0.144	0.118
Daily Adjustment	N	Y	Y	Y	Y	Y

Source: Johns Hopkins Coronavirus Resource Center and authors' calculations. $\Delta \ln(\text{Open}_t)$ and $\Delta \ln(\text{Close}_t)$ are the daily log changes in the opening (i.e., day $t - 1$ to day t open) and closing values of the Wilshire 5000. $\Delta \ln(C_t^{-2,-1})$ is the change in predicted cases. $\Delta \ln(C_t^{-2,-1})$ is the change in actual observed cases between days $t - 2$ and $t - 1$. $\Delta \ln(C_t^{-1,0})$ is the change in actual observed cases between days $t - 1$ and t . Robust standard errors in parenthesis. Columns 2-6 divide all variables by the number of days since the last observation (i.e. over weekends). Sample period is January 22 to April 10, 2020.

percent for closing and opening prices respectively. These effects are statistically significant at conventional levels.

In the second and subsequent columns of each table, we adjust the dependent and independent variables by the number of days since the last trading day. This adjustment insures that changes which transpire across weekends and holidays, when markets are closed, are not spuriously large compared to those that take place across successive calendar days. As indicated in the second column of each table, relationships remain statistically significant at conventional levels and now have the interpretation of daily growth rates. Here, a doubling of predicted cases per day leads to average declines of 8.6 percent for closing and 4.8 percent for opening prices.

In column 3 of each table, we examine whether the explanatory power of $\Delta C_t^{-2,-1}$ remains after controlling for a simple, local proxy of outbreak severity, the most recent change in reported cases. We use a slightly different variable in each table to account for the timing of the opening and closing returns. For the opening price regressions, we use $\Delta \ln(C_t^{-2,-1})$ under the assumption that the only information available to predict the opening price on day t is the difference in reported cases from days $t - 2$ and $t - 1$. For the closing price regressions, however, we use $\Delta \ln(C_t^{-1,0})$ to informally allow for the possibility that, although day t cases are not officially available until after closing, some information might "leak out" during day t trading.

In both cases, these measures are positive but not statistically significant at conventional levels. Moreover, they have little impact on our coefficients of interest. These results suggest that the primary role local increases in reported cases play in determining market value is through their contribution to the overall sequence of reported infections, manifest in the estimated model

Table 2: Change in Predicted COVID-19 Cases ($\widehat{\Delta C_t^{-2,-1}}$) vs Market Close Returns

	(1) $\Delta \ln(\text{Close})$	(2) $\Delta \ln(\text{Close})$	(3) $\Delta \ln(\text{Close})$	(4) $\Delta \ln(\text{Close})$	(5) $\Delta \ln(\text{Close})$	(6) $\Delta \ln(\text{Close})$
$\Delta \ln(C_t^{-2,-1})$	-0.067** (0.030)	-0.080** (0.030)	-0.089*** (0.031)	-0.093*** (0.034)	-0.146*** (0.041)	-0.089*** (0.032)
$\Delta \ln(C_t^{-1,0})$			0.033 (0.031)	0.055 (0.037)	0.065* (0.035)	0.034 (0.032)
$I(\Delta SIndex)$				-0.021 (0.018)		
$\Delta \ln(SIndex)$					-0.091 (0.076)	
Fiscal Stimulus						-0.005 (0.018)
Constant	-0.009 (0.006)	-0.005 (0.005)	-0.010** (0.004)	-0.010** (0.004)	-0.010** (0.004)	-0.010** (0.004)
Observations	47	47	47	47	43	47
R^2	0.092	0.086	0.103	0.145	0.224	0.104
Daily Adjustment	N	Y	Y	Y	Y	Y

Source: Johns Hopkins Coronavirus Resource Center and authors' calculations. $\Delta \ln(\text{Open}_t)$ and $\Delta \ln(\text{Close}_t)$ are the daily log changes in the opening (i.e., day $t - 1$ to day t open) and closing values of the Wilshire 5000. $\Delta \ln(\widehat{C_t^{-2,-1}})$ is the change in predicted cases for day t using information from days $t - 1$ and $t - 2$. $\Delta \ln(C_t^{-2,-1})$ is the change in actual observed cases between days $t - 2$ and $t - 1$. $\Delta \ln(C_t^{-1,0})$ is the change in actual observed cases between days $t - 1$ and t . Robust standard errors in parenthesis. Columns 2-6 divide all variables by the number of days since the last observation (i.e. over weekends). Sample period is January 22 to April 10, 2020.

parameters.

In the final three columns of Tables 1 and 2 we examine the robustness of our results to including coarse controls for policy. As the COVID-19 pandemic has unfolded in the United States, state and local governments as well as the federal government have undertaken various measures to control its spread and limit the economic burden the disease itself imposes. Enactment of such policies is by definition correlated with the severity of the outbreak, and some of them may be designed to stabilize equity markets, confounding our results.

We consider two controls for policy. The first is a country-level index developed at Oxford University, the Government Response Stringency Index (SIndex), which tracks travel restrictions, trade patterns, school openings, social distancing and other such measures, by country and day.¹⁹ We make use of this index in two ways in columns 4 and 5 of Tables 1 and 2. First, we include an indicator function $I\{\Delta SIndex\}$ which takes a value equal to one if the index changes on day t . Second, we use log changes in the index itself, $\Delta \ln(SIndex)$. As indicated in the tables, neither covariate is statistically significant at conventional levels, and their inclusion has little impact on the coefficient of interest.

Our second control for policy is a coarse measure of fiscal stimulus. This dummy variable is set to one for four days (chosen by the authors) upon which major fiscal policies were enacted. The “Coronavirus Preparedness and Response Supplemental Appropriations Act, 2020”, which appropriated 8.3 billion dollars for preparations for the COVID-19 outbreak, was signed into law on March 6. Then, from March 25 to March 27, Congress voted for and the President signed into

¹⁹This index can be downloaded from <https://www.bsg.ox.ac.uk/research/research-projects/oxford-covid-19-government-response-tracker>.

law the 2 trillion dollar “Coronavirus Aid, Relief, and Economic Security Act.” As reported in the table, this dummy variable, too, is statistically insignificant at conventional levels, and exerts no influence on the coefficient of interest.

Policy variables’ lack of statistical significance is somewhat puzzling. One explanation for this outcome is that these measures are a function of the information contained in the cumulative reported cases, and therefore retain no independent explanatory power. On the other hand, the various government policies included in the SIndex may have offsetting effects. For example, while social distancing measures might be interpreted by the market as a force that reduces the economic severity of the crisis, they may also be taken as a signal that the crisis is worse than publicly available data suggest. At present, we do not have the degrees of freedom to explore the impact of individual elements of the this index, but plan to do so in a future draft when inclusion of additional countries in the analysis allows for panel estimation.

3.3 Firm-Level US Returns During COVID-19

In this section we examine the relationship between unanticipated changes in predictions and returns at the firm level using the OLS regression

$$R_{jt} = \delta + \beta_j^{C^{-2,-1}} * \Delta \ln \left(\widehat{C_t^{-2,-1}} \right) + \beta_j^{MKT} * \Delta \ln (Index_t) + \epsilon_t, \quad (5)$$

where the dependent variable is the daily return of firm j on day t . The second term on the right-hand side accounts for the possibility that COVID-19 is no different than any other aggregate shock, and that a firm’s return during the pandemic merely reflects its more general co-movement with the market (Sharpe, 1964b). When this term is included, $\beta_j^{C^{-2,-1}}$ represents the firm’s return in excess of its covariance with the market.

The sample period is January 22 to April 10, 2020. Data are taken from Bloomberg and Yahoo finance.²⁰ In the analysis that follows, we focus on the sample of 4070 firms incorporated in the United States for which we observe returns during the sample period. These firms span 505 six-digit NAICS classifications and 249 4-digit NAICS classifications.

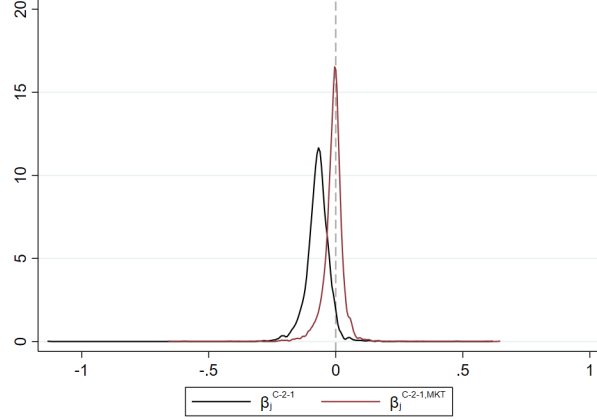
We run this regression separately for each firm j , yielding 4070 estimates. Their distribution is summarized in the kernal density reported in Figure 8. In black, we plot the distribution of $\widehat{\beta_j^{C-2,-1}}$, the measure of exposure from the regression that does not control for the market index. Intuitively, given the behavior of the overall market discussed above, we find that the overwhelming majority of $\widehat{\beta_j^{C-2,-1}}$ are below zero, indicating that firms’ returns generally have a negative relationship with predicted increases in cumulative infections. In red, we plot the distribution of $\widehat{\beta_j^{C-2,-1|MKT}}$, our notation for the measure of exposure estimated in the presence of the market index. While the bulk of exposures remain negative, the distribution shifts clearly to the right.²¹

The left panel of Figure 9 summarizes firms’ exposure to COVID-19 by two-digit NAICS sector. While sectors clearly vary in (and are sorted by) their median level of exposure, there is substantial variation across firms within sectors. The right panel of the figure plots firms’ average exposure by sector against their average daily returns between January 17, the last trading day prior to the

²⁰We use Yahoo for stock prices, as we lost immediate access to Bloomberg terminals on March 18. We use the Bloomberg data to filter our Yahoo sample as follows. We match firms by ticker from January, 22 to March 18. If returns from the two sources differ by 0.01 on more than one day, or if they differ by more than 1 on any day, we deem that firm’s returns unreliable and drop them from the analysis. The remaining returns have an in-sample correlation of 99.6 percent during the overlap period.

²¹96 percent of $\widehat{\beta_j^{C-2,-1}}$ are negative, while 65 percent of $\widehat{\beta_j^{C-2,-1|MKT}}$ are below zero.

Figure 8: Distribution of US Firms’ Sensitivity to COVID-19: $\widehat{\beta}_j^{C^{-2}-1}$ vs $\widehat{\beta}_j^{C^{-2}-1|MKT}$



Source: Johns Hopkins Coronavirus Resource Center, Bloomberg, Yahoo Finance and authors’ calculations. Figure reports the distribution of firm sensitivities to unanticipated changes in exponential model predictions, $\Delta\widehat{C}_t^{C^{-2}-1}$, estimated using equation 5. $\widehat{\beta}_j^{C^{-2}-1}$ measures total firm exposure while $\widehat{\beta}_j^{C^{-2}-1|MKT}$ removes “typical” co-movement with the market. Sample period is January 22 to April 10, 2020.

United States’ first case, and April 10. We compute a firm’s mean daily return over this period, \bar{R}_j , where the bar denotes an average, as the geometric mean of its daily returns, R_{jt} .

All sectors exhibit a negative average return in response to the COVID-19 shock. Firms producing products more conducive to virus transmission (and therefore more heavily affected by the imposition of social distancing) – Accommodations, Entertainment, and Transportation – exhibit more negative values for $\widehat{\beta}_j^{C^{-2}-1}$ and relatively larger declines in daily average returns. The position of Mining, in the extreme lower left position of the figure, is also unsurprising given the implications of the sharp contraction in US economic activity on energy use.²² Agriculture, Utilities, Education, Professional Services and FIRE (Finance, Insurance and Real Estate) are towards the upper right of the figure. These sectors are less exposed to COVID-19 due either to their necessity or their ability to conduct business online, and experience relatively less negative average returns.

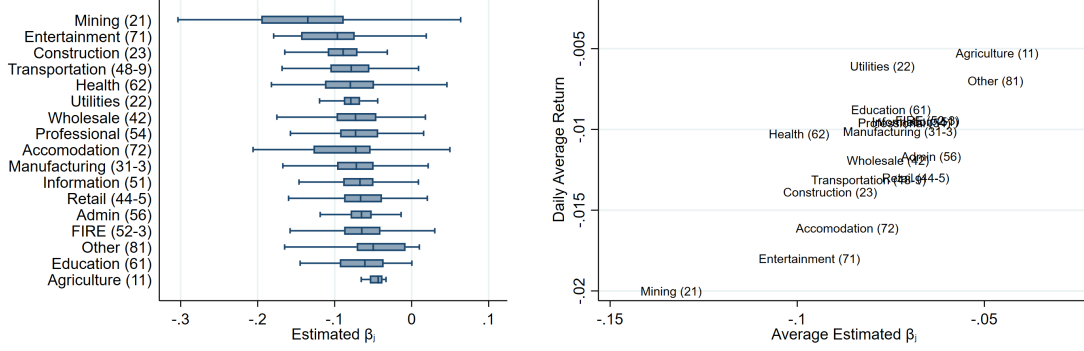
Table 3 investigates the correlates of exposure to COVID-19 by regressing $\widehat{\beta}_j^{C^{-2}-1}$ on a series of firms’ pre-pandemic attributes: total assets ($Assets_j$), total assets less property, plant and equipment ($Assets_j^{IPPE}$), PPE, employment (Emp), operating profit ($OpProfit$), cash and debt.²³ For ease of interpretation, all independent variables have been converted to z-scores, so that coefficients are in units of standard deviations of the dependent variable.

Coefficient estimates in the first column of the table indicate that $\widehat{\beta}_j^{C^{-2}-1}$ is more negative for firms with greater assets and PPE, and more positive for firms with larger employment and operating profit. Each of these coefficients is statistically significant at conventional levels. In column 2 (and for the remainder of the table), we net PPE out of total assets and find that while its explanatory power dissipates, the signs on PPE, employment and operating profit remain the

²²Returns in mining, which include oil and gas extraction, are also affected by recent disagreements within OPEC, which are potentially endogenous to the pandemic.

²³Firm attributes are from Compustat for the latest reporting period available, the fourth quarter of 2019. We match firms to balance sheet information in Compustat via their CUSIP numbers.

Figure 9: US Firms' Sensitivity to COVID-19 ($\widehat{\beta}_j^C$), by NAICS Sector



Source: Johns Hopkins Coronavirus Resource Center, Bloomberg, Yahoo Finance and authors' calculations. Figure reports the distribution of firm sensitivities ($\widehat{\beta}_j^C$) to unanticipated changes in exponential model projections, $\Delta C_t^{(-2,-1)}$, estimated using equation 5. Geometric average of daily returns calculated from January 17 - April 10, 2020.

Table 3: Firm Attributes and COVID-19 Exposure ($\widehat{\beta}_j^{C-2-1}$)

	(1)	(2)	(3)	(4)	(5)	(6)	(7)
	$\widehat{\beta}_j^{C-2-1}$						
$Ln(Assets_j)$	-0.0053** (0.002)						
$Ln(Assets_j^{PPE})$		-0.0015 (0.002)	0.0003 (0.002)	0.0037* (0.002)	-0.0004 (0.002)	0.0069*** (0.002)	0.0040 (0.003)
$Ln(PPE_j)$	-0.0101*** (0.003)	-0.0066*** (0.002)	-0.0060** (0.002)	-0.0042 (0.003)	-0.0077*** (0.002)	-0.0029 (0.003)	0.0059* (0.004)
$Ln(Emp_j)$	0.0098*** (0.002)	0.0042* (0.002)	0.0040* (0.002)	0.0045** (0.002)	0.0053** (0.002)	0.0041* (0.002)	-0.0000 (0.003)
$Income_j$	0.0034*** (0.001)	0.0026*** (0.001)	0.0027*** (0.001)	0.0024*** (0.001)	0.0025*** (0.001)	0.0026*** (0.001)	0.0020*** (0.001)
$Ln(Cash_j)$				-0.0026 (0.002)			-0.0042** (0.002) -0.0056*** (0.002)
$Ln(Debt_j)$					-0.0069*** (0.002)		-0.0073*** (0.002) -0.0063*** (0.002)
Constant	-0.0773*** (0.001)	-0.0749*** (0.001)	-0.0744*** (0.001)	-0.0775*** (0.001)	-0.0764*** (0.001)	-0.0771*** (0.001)	-0.0758*** (0.001)
Observations	2615	2305	2277	1842	1815	1815	1790
R^2	0.026	0.009	0.009	0.017	0.010	0.019	0.175
NAICS-4 FE	N	N	N	N	N	N	Y

Source: Johns Hopkins Coronavirus Resource Center, Bloomberg, Yahoo Finance, Compustat and authors' calculations. Table reports results of cross-sectional OLS regression of firms' estimated exposure to COVID-19 from equation 6, $\widehat{\beta}_j^{C-2-1}$, on their pre-pandemic levels of total assets, total assets less property, plant and equipment ($Assets_j^{PPE}$), PPE, employment, operating profit, cash and debt. Firm attributes are from Compustat for the latest reporting period available, the fourth quarter of 2019. Robust standard errors reported in parenthesis below coefficients.

same. One explanation for the result with respect to PPE is that investors are more apt to bid down the stock prices of capital-intensive firms that cannot reduce costs during the pandemic. To the extent that firms find it easier to furlough workers than shed their fixed assets, the market

values of labor-intensive firms will fall relatively less.

In columns 3 and 4, we add two firm attributes, cash and debt, intended to capture key elements of firm's capital structure that may affect survival during the pandemic. As indicated in the table, results are similar with the addition of cash. In column 4, however, PPE becomes marginally significant with the addition of debt, indicating that it may be firms with large capital stocks financed by debt that is the key determinant of firms' exposure. Such a relationship is consistent with the findings of [Ramelli and Wagner \(2020\)](#), who also emphasize the constraining role that debt may play during the economic downturn that accompanies a severe pandemic. As information on firm debt is not available for approximately 400 firms, we re-estimate in column 5 the specification from column 2 for the subset of firms for which debt is available. Results are similar.

In columns 6 and 7 we include all covariates in the regression without, and then with, four-digit NAICS fixed effects. Results are similar in both cases, with the exception of coefficient on employment becoming insignificant and the sign on PPE coefficient flipping from negative to positive. The latter may reflect the fact that, after controlling for firm's debt and the overall capital intensity of the firm's sector (via their fixed effects), larger firms are estimated to have less negative exposure to COVID-19. We note that the R^2 of this regression increases substantially with the inclusion of industry fixed effects, suggesting firms' primary industries contain substantial information about their exposure.

Having identified key channels of firm exposure to COVID-19, we assess the quantitative importance of this exposure in firms' returns over the sample period using a cross-sectional OLS regression,

$$\bar{R}_j = \nu_1 \widehat{\beta_j^{C-2-1}} + \nu_2 \widehat{\beta_j^{MKT}} + \xi_j. \quad (6)$$

Here, as above, \bar{R}_j is the geometric average of firm j 's return from January 22 to April 10, and $\widehat{\beta_j^{C-2-1}}$ and $\widehat{\beta_j^{MKT}}$ are its exposures to the log changes in predicted cumulative infections and the US market index (Wilshire 5000) estimated in equation 5. To the extent that exposure to COVID-19 influences firm returns beyond their co-movement with the market, both terms in equation 6 are expected to have explanatory power.²⁴

Results are reported in Table 4, where the first column focuses solely on firms' sensitivity to COVID-19, and the second column includes both exposures. The coefficient estimate in column 1, 0.050, implies that a one standard deviation increase in $\widehat{\beta_j^{C-2,-1}}$ is associated with a 0.33 standard deviation reduction in average daily returns, a sizable influence.²⁵ The estimate for $\widehat{\beta_j^{C-2,-1}}$ in column 2 indicate that this influence remains even after accounting for firms' sensitivity to the market (which as noted above is also directly impacted by COVID-19). Here, the magnitude of the coefficient, 0.023, implies that a one standard deviation increase in exposure to COVID-19 is associated with a 0.11 standard deviation decrease in daily returns, or roughly one quarter of the magnitude of the implied impact of a standard deviation change in market exposure.

²⁴This regression similar in spirit to those proposed by [Fama and MacBeth \(1973\)](#), though here we use a single cross section rather than repeated cross sections, i.e., one for each day as the crisis unfolds. We plan to exploit the panel nature of our data in a future draft.

²⁵The standard deviations of \bar{r}_j , $\widehat{\beta_j^{C-2-1}}$ and $\widehat{\beta_j^{MKT}}$ are 0.008, 0.051 and 0.043.

Table 4: Average Firm Returns and COVID-19 ($\widehat{\beta_j^{C-2,-1}}$) vs Market Exposure ($\widehat{\beta_j^{MKT}}$)

	R_j	\overline{R}_j
$\widehat{\beta_j^{C-2,-1}}$	0.050*** (0.008)	0.023*** (0.007)
$\widehat{\beta_j^{MKT}}$		-0.007*** (0.001)
Constant	-0.006*** (0.001)	-0.003*** (0.001)
Observations	4070	4070
R^2	0.114	0.198

Source: Johns Hopkins Coronavirus Resource Center, Bloomberg, Yahoo Finance and authors' calculations. Table reports results of cross-sectional OLS regression of firms' average return between January 22 and April 10, \overline{r}_j , on $\widehat{\beta_j^C}$ and $\widehat{\beta_j^{MKT}}$, the coefficient estimates from equation 5. Robust standard errors reported in parenthesis below coefficients. The standard deviations of \overline{r}_j , $\widehat{\beta_j^C}$ and $\widehat{\beta_j^{MKT}}$ are 0.008, 0.051 and 0.043.

3.4 Spatial Implications and Employment

In this section we examine whether the US stock markets' reactions to COVID-19's forecast changes in employment at the regional level.²⁶ Job loss is a major concern of both workers and public officials; an ability to predict employment declines by industry and region may be aid in developing policy responses.²⁷

For each US county c , we construct the average change in market value from January 22 to April 10 as the employment-share weighted change in the market value of its constituent four-digit NAICS industries (n) as

$$\Delta \ln(\widehat{MV}_c) \equiv \sum_{n \in N} \frac{E_{nc}}{E_c} * \Delta \ln(\widehat{MV}_n). \quad (7)$$

where E_{nc} is the 2016 employment in county c in industry n , and $\Delta \ln(MV_n)$ is the log change in market value of all firms in n attributable to COVID-19 exposure.²⁸ As illustrated in Figure 10,

²⁶As firm employment in COMPUSTAT is updated quarterly, we are at present unable to examine the link between firm exposure to COVID-19 and firm employment directly. An additional complication is that firm employment data in COMPUSTAT reflects worldwide, not just US employment. We will include this analysis as the data become available.

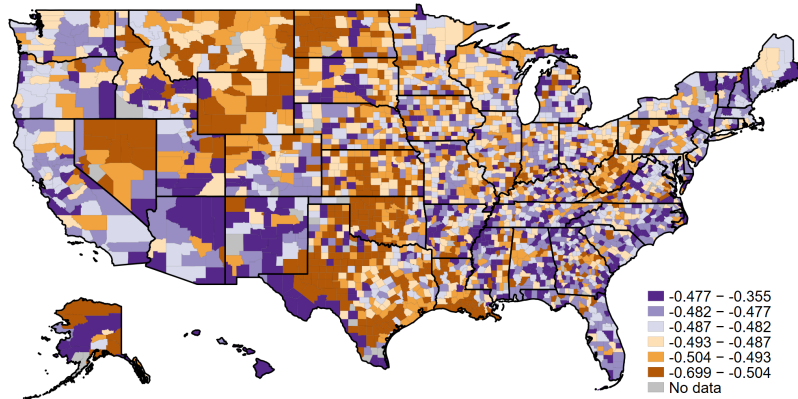
²⁷We perform two checks on the representativeness of the publicly listed firms in our sample with respect to employment. First, in appendix Figure A.5, we show that employment among these firms, while obviously different in levels, is highly correlated across industries with US employment in 2016. Second, we find, in appendix Figure A.6, that 95 percent of all counties have at least 76 percent of their employment in industries appearing among publicly listed firms.

²⁸Country business pattern employment for 2016 are the latest available from Eckert et al. (2020). We show in appendix Figures A.4 and A.4 that industries with greater capital intensity exhibit greater declines in market value.

$\Delta \ln(\widehat{MV}_n) = \ln \left(\frac{\sum_{j \in n} MV_{j,t_0}(1+\hat{\tau})^{52}}{MV_{n,t_0}} \right)$ is the market capitalization weighted average of return of all firms j in

counties vary substantially in their weighted average changes in market value. Notably, much of the “oil belt”, from Texas and Louisiana up through Oklahoma into Wyoming and North Dakota, and parts of Pennsylvania – in brown – exhibit the largest declines. By contrast, much of California and the East Coast – in blue – feature relatively lower declines. Interpreted through the lens of Table 3, these trends indicate that the coasts have disproportionately large employment in industries containing labor-intensive firms.

Figure 10: Employment Weighted Change in Market Value, by County



Source: Johns Hopkins Coronavirus Resource Center, Bloomberg, Yahoo Finance, Compustat, [Eckert et al. \(2020\)](#) and authors’ calculations. We omit counties (in grey) if we match less than 70% of their employment at the NAICS-4 level. This is under 5% of all counties.

Thus far, official estimates of job loss during the pandemic are available only in terms of initial unemployment claims from the US Department of Labor, and only at the state level.²⁹ Figure A.7 displays the relationship between state changes in market value between January 22 and April 10 (constructed in a manner analogous to counties above), and new jobless claims per worker. That is, we sum the initial jobless claims from March 18 (before most of the COVID-19 labor market disruption began) to April 11, and divide by the initial number of employees in the state according to the 2016 CDP.

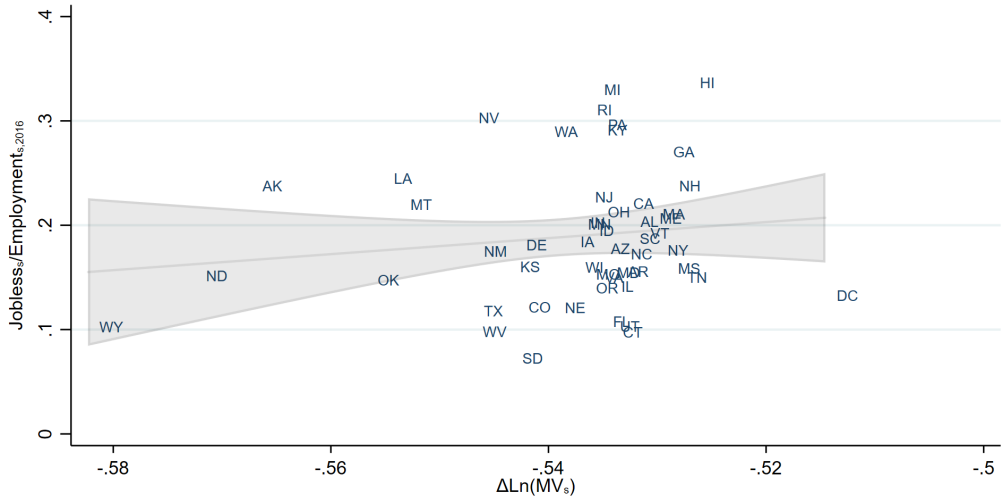
As reported in the figure, states whose employment is more concentrated in industries with smaller market value losses exhibit *greater* growth in jobless claims per worker. As market value declines are greater in more labor-intensive industries (Figure A.5), this trend is consistent with the idea that the labor-intensive sectors favored by the market shed relatively more workers compared to firms in capital-intensive sectors in an effort to cut costs as consumption contracts across the board ([Baker et al., 2020](#)) and revenues decline. Given the unprecedented contraction in global economic activity, capital-intensive firms’ property, plant and equipment is effectively sunk. As a consequence, firms in these industries that retain leverage on these assets may fare better by continuing to employ workers, producing at a loss given the decline in demand, so long as they are able to cover short-run variable costs.

We investigate this mechanism more formally using an OLS difference-in-differences (DID) regression,

industry n .

²⁹Initial jobless claims are available from the US Department of Labor website at https://oui.dolleta.gov/unemploy/claims_arch.asp. Current Employment Survey (CES) data available from the Bureau of Labor Statistics (BLS) is not yet available for March, but will be included in a future draft.

Figure 11: Jobless Claims per Worker vs. State-Average Change in Market Value



Source: Johns Hopkins Coronavirus Resource Center, Bloomberg, Yahoo Finance, Compustat, [Eckert et al. \(2020\)](#), US Department of Labor and authors' calculations.

$$\frac{Jobless_{sw}}{E_{s,2016}} = \eta_0 + \eta_1 Post * \Delta \ln(\widehat{MV}_s) + \eta_2 Post * X_s + \eta_3 \Gamma_{sw} + \rho_w + \rho_s + \epsilon_{sw}, \quad (8)$$

where the dependent variable is the ratio of jobless claims in state s in week w expressed in percentage terms, X_s are state labor market characteristics (defined below), Γ_{sw} are week-varying state controls, and the last two terms are state and week fixed effects. We define the treatment period ($Post$) as the full weeks following the official March 11 announcement by the WHO declaring COVID-19 a global pandemic.³⁰ During the pre-period, average jobless claims per worker across states is 0.2 percent; after March 11, they jump to 4.7 percent. For ease of interpretation covariates have been standardized so the coefficients may be interpreted as the effect of increasing the covariate by one standard deviation. Standard errors are clustered at the state level.

Results are reported in Table 5. In column 1, we include only state and week fixed effects and the DID term of interest, $\Delta \ln(\widehat{MV}_s) * Post$. The coefficient estimate, indicates that a 1 standard deviation increase in market value is associated with 0.38 percentage point increase in jobless claims per worker per week in the post period, relative to the pre-period. This effect is sizable, representing 10 percent of the average post-period increase.

In column 2 we include the share of state employment amenable to teleworking from home developed by [Dingel and Neiman \(2020\)](#).³¹ The estimated coefficient on this variable is intuitive: the more intensive a state is in work that can be done at home, the lower the initial jobless claims. Inclusion of this covariate raises the magnitude of the DID term of interest to 0.52.

The third column in Table 5 introduces a covariate capturing the staggered stay-at-home orders imposed by states during the post period.³² Predictably, the coefficient for this variable is large in magnitude and statistically significant at conventional levels. Its sign indicates that the roll-out

³⁰ As illustrated in appendix Figure A.7, there is a substantial break in jobless growth following the WHO announcement, indicated by the red vertical line in the figure.

³¹ As with the dependent variable in this regression, we compute this measure as the employment-weighted average teleworking share across 4-digit NAICS industries.

³² Data collected from “State Data and Policy Actions to Address Coronavirus,” provided by the Henry J Kaiser Family Foundation.

Table 5: Jobless Claims and Market Valuation

	(1) $\frac{Jobless_{s,w}}{Emp_{s,2016}}$	(2) $\frac{Jobless_{s,w}}{Emp_{s,2016}}$	(3) $\frac{Jobless_{s,w}}{Emp_{s,2016}}$	(4) $\frac{Jobless_{s,w}}{Emp_{s,2016}}$	(5) $\frac{Jobless_{s,w}}{Emp_{s,2016}}$	(6) $\frac{Jobless_{s,w}}{Emp_{s,2016}}$
$\Delta \ln(\widehat{MV}_s)$	0.3792* (0.203)	0.5178** (0.215)	0.4292** (0.202)	0.4330** (0.206)	0.4629** (0.204)	0.3533* (0.207)
Teleworkable _s		-0.3850* (0.218)	-0.4176* (0.208)	-0.4148* (0.208)	-0.5410* (0.269)	-0.5273* (0.273)
I(Stay Order _{s,t})			1.0636*** (0.380)	1.0685*** (0.382)	1.0283*** (0.371)	1.0923*** (0.372)
Ln(Employment ₂₀₁₆)				-0.0153 (0.217)	0.0185 (0.224)	0.0318 (0.230)
× Post						
Workforce Match _s					-0.2106 (0.216)	-0.1774 (0.212)
× Post						
Constant	0.2236*** (0.056)	0.2236*** (0.055)	0.2236*** (0.052)	0.2236*** (0.052)	0.2236*** (0.052)	0.2236*** (0.052)
Shortened $\beta_j^{C-2,-1}$ Estimation	N	N	N	N	N	Y
State FE	Y	Y	Y	Y	Y	Y
Week FE	Y	Y	Y	Y	Y	Y
Observations	765	765	765	765	765	765
R ²	0.835	0.840	0.846	0.846	0.848	0.845

Source: Johns Hopkins Coronavirus Resource Center, Bloomberg, Yahoo Finance, Henry J Kaiser Family Foundation, ([Eckert et al., 2020](#)) and authors' calculations. $\Delta \ln(\widehat{MV}_s)$ is the employment weighted average change in industry market n value at the state level. Post is equal to 1 for full weeks after March 11. Standard errors are clustered at the state level. Independent variables are in terms of standard deviations.

of social mobility restrictions coincides with increases in jobless claims per worker conditional on the share of work that can be done from home. In this specification, the DID coefficient of interest remains positive and statistically significant, with a magnitude of 0.43.

Columns 4 and 5 of Table 5 investigate whether the DID term of interest is sensitive to including two additional controls, for total employment in the state, interacted with *Post*, and the share of state workforce for which we observe a 4-digit NAICS industry. Neither covariate is statistically significant at conventional levels, and the magnitude of the DID term of interest remains within the bounds established by previous columns.

As it is possible that equity market reactions are themselves a function of states' exposure to the rise in jobless claims, in the last column of Table 5 we restrict estimation to the period before March 18, the date of the first substantial increase in jobless claims. While the DID term of interest is estimated less precisely, it remains within the range of estimates in the earlier columns of the table.

Overall, the findings in Table 5 provide a consistent message: investors bid down the stock prices of firms less the more they are able to shed costs, and states intensive in these firms see greater initial jobless claims. During a pandemic, equity market participants appear to love precisely what labor market participants loathe – the ease with which workers can be temporarily furloughed or permanently dismissed.

4 Application to SARS

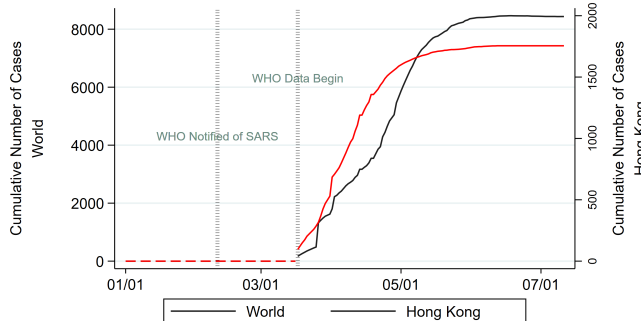
In this section we demonstrate historical precedent for the link between US stock market returns and COVID-19 discussed above by reporting a similar link during the Severe Acute Respiratory Syndrome (SARS) outbreak in Honk Kong nearly 20 years earlier.

The first SARS case was identified in Foshan, China in November 2002, but was not recognized as such until much later. According to [WHO \(2006\)](#), on February 10, 2003 a member of the WHO in China received an email asking:

“Am wondering if you would have information on the strange contagious disease (similar to pneumonia with invalidating effect on lung) which has already left more than 100 people dead in ... Guangdong Province, in the space of 1 week. The outbreak is not allowed to be made known to the public via the media, but people are already aware of it (through hospital workers) and there is a ‘panic’ attitude.”

The WHO immediately began an investigation into SARS, and started releasing regular reports of suspected and confirmed cases beginning March 17, 2003.³³ The World Health Organization (WHO) declared SARS contained in July 2003, though cases continued to be reported until May 2004. Figure 12 plots the cumulative number of confirmed SARS infections worldwide (left scale) and in Hong Kong (right scale). The two vertical lines in the figure note the days on which the WHO officially received the aforementioned email, and the first day on which the WHO began reporting the number of infections on each weekday.

Figure 12: SARS Infections in Hong Kong and Worldwide During 2003



Source: World Health Organization and authors' calculations. Figure displays the cumulative reported SARS infections in Hong Kong and the rest of the world from January 1, 2003 to July 11, 2003. The two vertical lines in the figure note the days on which the WHO officially received the aforementioned email, and the first day on which the WHO began reporting the number of infections on each weekday.

Hong Kong and China accounted for the vast majority of cases worldwide.³⁴ We focus our analysis on Hong Kong for two reasons related to data reliability. First, while China acknowledged having over 300 cases of “atypical pneumonia” in February, the Ministry of Health did not provide day-by-day counts until March 26. In fact, on March 17, the day before WHO began releasing daily situation reports, Chinese authorities informed the WHO that “[t]he outbreak in Guangdong

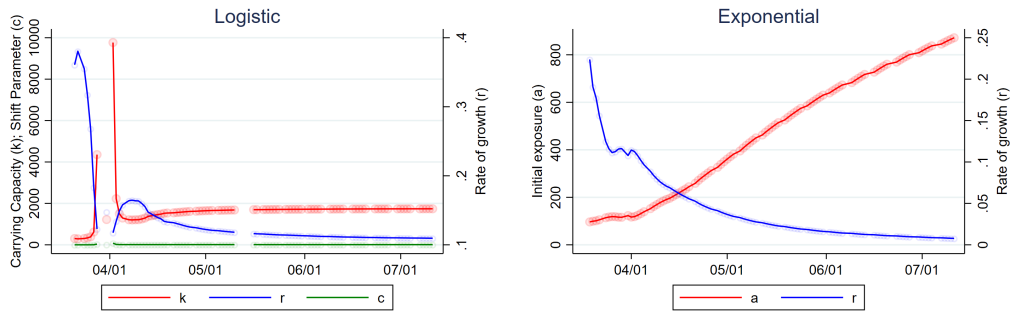
³³Counts were released every weekday. These data can be downloaded from <https://www.who.int/csr/sars/country/en/>. A timeline of WHO activities related to SARS events can be found at https://www.who.int/csr/don/2003_07_04/en/.

³⁴Reported cases for China are plotted in appendix Figure A.2.

is said to have tapered off.” The next day, cases were reported in 8 locations other than China – including Hong Kong. When China did begin reporting daily counts, on March 26, the first count was 800 cases. This large initial level of infections accounts for the sharp jump in world counts displayed for that day in Figure 12. Lack of real-time infection updates in mainland China prior to this jump undermines reliable estimation of model parameters, thereby impeding accurate assessment of unanticipated changes in infections. Second, it is unclear how China’s restrictions on foreign ownership of companies’ “A shares” during this period affects the extent to which such unanticipated changes will be reflected in Mainland firms’ equity value.

We estimate equations 1 and 2 by day for each country as discussed in Section 2. The daily parameter estimates for the logistic estimation, \hat{k}_t , \hat{c}_t and \hat{r}_t are displayed graphically in the left panel of Figure 13. The right panel displays analogous estimates for the exponential function. Gaps in either panel’s time series represent lack of convergence. As indicated in the figure, logistic parameters fail to converge for several days early in the outbreak, and then once again when the estimates have started to settle down in the beginning of May. The exponential model, by contrast, converges on every day in the sample period.

Figure 13: Parameter Estimates for SARS



Source: World Health Organization and authors’ calculations. The left panel plots the sequence of logistic parameters, \hat{k}_t , \hat{c}_t and \hat{r}_t , estimated using the information up to each day t on the cumulative reported cases for Hong Kong displayed in Figure 12. Right panel Figure plots the analogous sequence of exponential parameters, \hat{a}_{t-1} and \hat{r}_{t-1} , using the same data. Missing estimates indicate lack of convergence (see text). Circles represent estimates. Solid lines connect estimates.

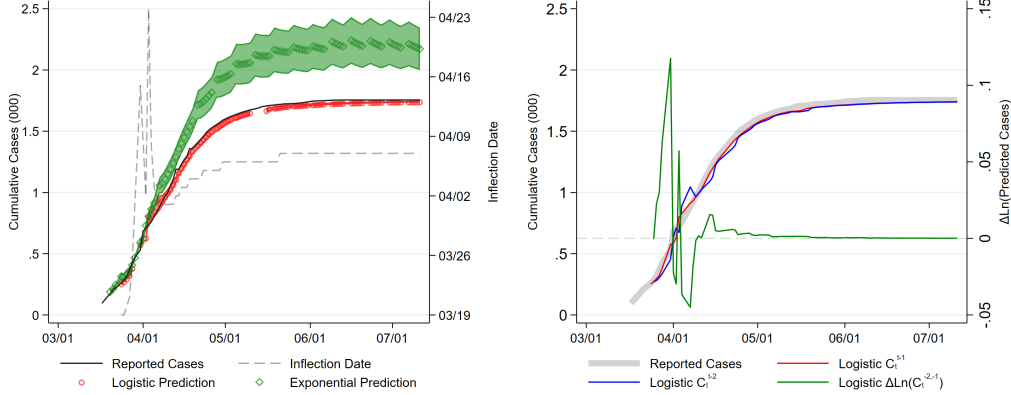
In the left panel of Figure 14, we compare the predictions of the two models. In each case, parameter estimates from day $t - 1$ are used to predict the cumulative number of cases for day t . Shading represents 95 percent confidence intervals. As indicated in the panel, predicted infections under the two models (left axis) are similar through the first week in April, but diverge thereafter. Interestingly, this divergence coincides with a stabilization of the estimated inflection point of the logistic curve (right axis), which, as illustrated by the dashed grey line in the panel, hovers between April 5 and 7 from April 5 onward.³⁵

We use the predictions of the logistic model for the remainder of the analysis. The right panel of Figure 14 compares the logistic model predictions for day t using information as of day $t - 1$, $\widehat{C_t^{t-1}}$, versus day $t - 2$, $\widehat{C_t^{t-2}}$, as well as the log difference between these predictions, $\Delta \ln(\widehat{C_t^{-2,-1}})$.³⁶ We find that $\Delta \ln(\widehat{C_t^{-2,-1}})$ exhibits wide swings in value during the early stages of the outbreak, before settling down in late April. As illustrated in Figure 15, these swings have a noticeably negative correlation with aggregate stock market performance in Hong Kong, as identified via daily

³⁵The inflection point is given by $\ln(\hat{c}_t)/\hat{r}_t$.

³⁶We use the last available parameter estimates for days on which logistic parameters do not converge.

Figure 14: Daily Predictions (\widehat{C}_t^{t-1}) for SARS



Source: World Health Organization and authors' calculations. Left panel displays predicted cumulative cases for each day t , \widehat{C}_t^{t-1} , information as of day $t-1$, based on parameter estimates reported in Figure 13. Shading spans 95 percent confidence intervals. Dashed line (right scale) traces out the estimated of the logistic curve's inflection point ($\ln(\widehat{c}_t)/\widehat{r}_t$). Right panel reports day t predicted cumulative cases under the logistic model using information as of day $t-1$, \widehat{C}_t^{t-1} , and day $t-2$, \widehat{C}_t^{t-2} , as well as the log difference between these predictions, $\Delta \ln(\widehat{C}_t^{-2,-1})$. Missing estimates in left panel indicate lack of convergence (see text).

log changes in the Hang Seng Index.³⁷

We explore this relationship formally in an OLS estimation of equation 4. Coefficient estimates and robust standard errors are reported in Table 6. In the first column, we find a negative and statistically significant relationship using the raw data displayed in Figure 15. In column 2, we account for weekends and holidays by dividing both the left- and right-hand side variables by the number of days over which the returns are calculated, so that the regression coefficient represents a daily change in market value for a given log change in predicted cases. Here, too, the coefficient estimate is negative and statistically significant at conventional levels, and higher in absolute magnitude.

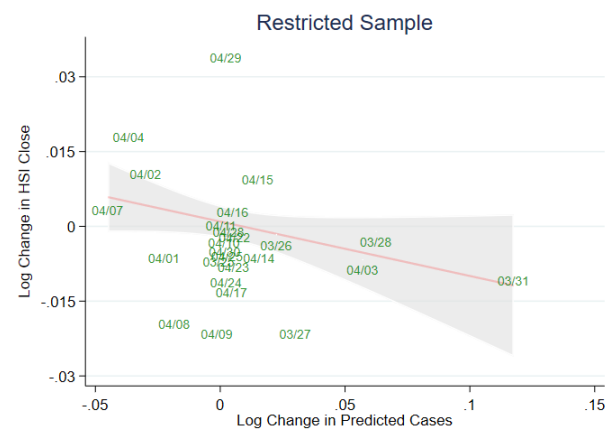
In column 3, we examine whether the explanatory power of $\Delta \ln(\widehat{C}_t^{-1,-2})$ remains after controlling for a simple, local proxy of outbreak severity, the difference in cumulative *reported* infections between days $t-1$ and $t-2$, $\Delta \ln(C_t^{-1,-0})$. As indicated in the table, the coefficient of interest remains negative and statistically significant at conventional levels, though of lower magnitude in absolute terms. The coefficient for $\Delta \ln(C_t^{-2,-1})$ is also negative and statistically significant.

Finally, in column 4, we repeat the specification for column 3 but include month fixed effects to account for potential secular movements in the market unrelated to SARS. Estimates are essentially unchanged.

Overall, the estimates in Table 6 suggest investors may have used simple epidemiological models to update their beliefs about the economic severity of the outbreak in Hong Kong, in real time. Across specifications, coefficient estimates indicate an average decline of 8 to 11 percent in response to a doubling of predicted cumulative infections.

³⁷Data for the Hang Seng index are downloaded from Yahoo Finance.

Figure 15: Changes in Predicted SARS Cases ($\widehat{\Delta C_t^{-2,-1}}$) vs Hang Seng Index Returns



Source: World Health Organization, Yahoo Finance and authors' calculations. Figure displays the daily log change in the Hang Seng Index against the daily log change in predicted cases for day t based on information as of day $t-1$ versus day $t-2$, $\Delta \ln(\widehat{C_t^{-2,-1}})$.

Table 6: Changes in Predicted SARS Cases vs Hang Seng Index Returns

	(1) $\Delta \ln(\text{Close})$	(2) $\Delta \ln(\text{Close})$	(3) $\Delta \ln(\text{Close})$	(4) $\Delta \ln(\text{Close})$
$\Delta \ln(\widehat{C_t^{-2,-1}})$	-0.0752*** (0.0241)	-0.1095*** (0.0396)	-0.0891** (0.0427)	-0.0923* (0.0537)
$\Delta \ln(C_t^{-2,-1})$			-0.0445** (0.0200)	-0.0483 (0.0294)
Constant	0.0018 (0.0013)	0.0010 (0.0011)	0.0019* (0.0011)	0.0025 (0.0051)
Daily Adjustment	N	Y	Y	Y
Month FE	N	N	N	Y
Observations	70	70	70	70
R^2	0.108	0.060	0.103	0.111

Source: World Health Organization, Yahoo Finance and authors' calculations. $\Delta \ln(\text{Close}_t)$ is the daily log change (i.e., day $t-1$ to day t) closing values Hang Seng Index. $\Delta \ln(\widehat{C_t^{-2,-1}})$ is the change in predicted cases for day t using information from days $t-1$ and $t-2$. $\Delta \ln(C_t^{-2,-1})$ is the change in reported cases between days $t-1$ and t . Robust standard errors in parenthesis. Columns 2-4 divide all variables by the number of days since the last observation (i.e. over weekends). Column 4 includes month fixed effects.

5 Conclusion

This paper shows that day-to-day changes in the predictions of standard models of infectious disease forecast changes in aggregate stock returns in Hong Kong during the SARS outbreak and the United States during the COVID-19 pandemic. In future updates to this paper, we plan to extend the analysis to other countries and pandemics, and to investigate the link between individual firms' returns and their exposure to public health crises via domestic and international input and output linkages as well as the demographics and occupations of their labor forces.

References

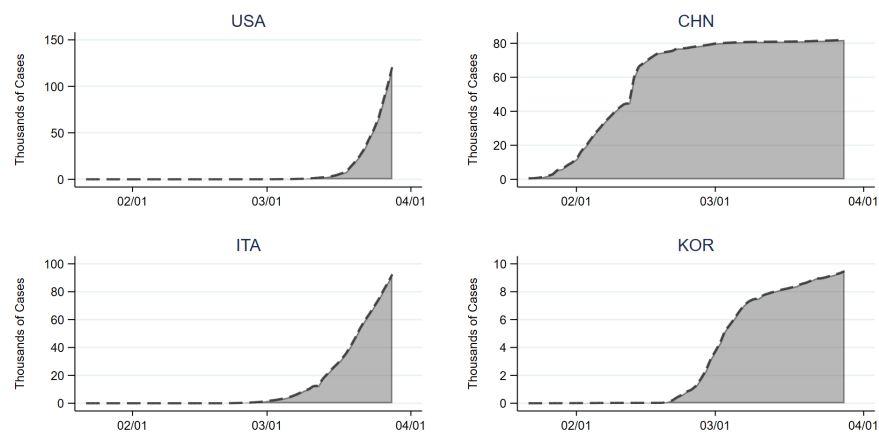
- Albuquerque, R. A., S. Yang, and C. Zhang (2020). Love in the time of covid-19: The resiliency of environmental and social stocks. *Working Paper*.
- Atkeson, A. (2020, March). What will be the economic impact of covid-19 in the us? rough estimates of disease scenarios. Working Paper 26867, National Bureau of Economic Research.
- Bai, H., K. Hou, H. Kung, E. X.N., and L. Zhang (2019). The CAPM Strikes Back? An Equilibrium Model with Disasters. *Journal of Financial Economics* 131(2), 269–298.
- Baker, S., N. Bloom, S. Davis, and S. J. Terry (2020). Covid-induced economic uncertainty. *NBER w26983*.
- Baker, S. R., N. Bloom, S. J. Davis, K. J. Kost, M. C. Sammon, and T. Viratyosin (2020, April). The unprecedeted stock market impact of covid-19. Working Paper 26945, National Bureau of Economic Research.
- Baker, S. R., R. Farrokhnia, S. Meyer, M. Pagel, and C. Yannelis (2020). How does household spending respond to an epidemic? consumption during the 2020 covid-19 pandemic. *NBER Working Paper 26949*.
- Ball, R. and P. Brown (1968). An empirical evaluation of accounting income numbers. *Journal of accounting research*, 159–178.
- Barro, R. J., J. F. Ursua, and J. Weng (2020, March). The coronavirus and the great influenza pandemic: Lessons from the “spanish flu” for the coronavirus’s potential effects on mortality and economic activity. Working Paper 26866, National Bureau of Economic Research.
- Bartik, A. W., M. Bertrand, Z. Cullen, E. L. Glaeser, M. Luca, and C. T. Stanton (2020). How are small businesses adjusting to covid-19? early evidence from a survey. *NBER w26989*.
- Bartik, T. J. (1991). Who Benefits from State and Local Economic Development Policies? *Upjohn Institute for employment Research*.
- Berger, D., K. Herkenhoff, and S. Mongey (2020). A seir infectious disease model with testing and conditional quarantine. *Working Paper*.
- Cajner, T., L. D. Crane, R. A. Decker, A. Hamins-Puertolas, and C. Kurz (2020). Tracking labor market developments during the covid-19 pandemic: A preliminary assessment. *Finance and Economics Discussion Series 2020-030*.
- Campbell, J. Y. and R. J. Shiller (1988). The dividend-price ratio and expectations of future dividends and discount factors. *The Review of Financial Studies* 1(3), 195–228.
- Coibion, O., Y. Gorodnichenko, and M. Weber (2020). Labor markets during the covid-19 crisis: A preliminary view. *NBER w27017*.
- Ding, W., R. Levine, C. Lin, and W. Xie (2020). Corporate immunity to the covid-19 pandemic. *Working Paper*.
- Dingel, J. I. and B. Neiman (2020). How many jobs can be done at home? *University of Chicago Mimeo*.

- Eckert, F., T. C. Fort, P. K. Schott, and N. J. Yang (2020). Imputing missing values in the us census bureau's county business patterns. Technical report, National Bureau of Economic Research.
- Fahlenbrach, R., K. Rageth, and R. M. Stultz (2020). How Valueable is Financial Flexibility When Revenue Stops? Evidence from the COVID-19 Crisis.
- Fama, E. and J. D. MacBeth (1973). Risk, return, and equilibrium: Empirical tests. *Journal of Political Economy*.
- Fama, E. F., L. Fisher, M. C. Jensen, and R. Roll (1969). The Adjustment of Stock Prices to New Information. *International Economic Review* 10.
- Fama, E. F. and K. R. French (1988). Dividend yields and expected stock returns. *Journal of financial economics* 22(1), 3–25.
- Gormsen, N. J. and R. S. Koijen (2020). Coronavirus: Impact on stock prices and growth expectations. *University of Chicago, Becker Friedman Institute for Economics Working Paper* (2020-22).
- Humphries, J. E., C. Neilson, and G. Ulyssea (2020). The evolving impacts of covid-19 on small businesses since the cares act. *working paper*.
- Kermack, W. O. and A. G. McKendrick (1927). A contribution to the mathematical theory of epidemics. *Proceedings of the royal society of london. Series A, Containing papers of a mathematical and physical character* 115(772), 700–721.
- Kermack, W. O. and A. G. McKendrick (1937). Contributions to the mathematical theory of epidemics iv. analysis of experimental epidemics of the virus disease mouse ectromelia. *Journal of Hygiene* 37(2), 172–187.
- Keynes, J. M. (1937). The general theory of employment. *The quarterly journal of economics* 51(2), 209–223.
- Knight, F. H. (1921). Risk, uncertainty and profit. *Library of Economics and Liberty*.
- Li, R., S. Pei, B. Chen, Y. Song, T. Zhang, W. Yang, and J. Shaman (2020). Substantial undocumented infection facilitates the rapid dissemination of novel coronavirus (sars-cov2). *Science*.
- Piguillem, F. and L. Shi (2020). The optimal covid-19 quarantine and testing policies. *Working Paper*.
- Ramelli, S. and A. F. Wagner (2020). Feverish stock price reactions to covid-19. *Swiss Finance Institute Research Paper* (20-12).
- Richards, F. J. (1959, 06). A Flexible Growth Function for Empirical Use. *Journal of Experimental Botany* 10(2), 290–301.
- Ross, R. (1911). *The Prevention of Malaria*. John Murray.
- Ru, H., E. Yang, and K. Zou (2020). What do we learn from sars-cov-1 to sars-cov-2: Evidence from global stock markets. *Working Paper*.
- Sharpe, W. F. (1964a). Capital Asset Prices: A Theory of Market Equilibrium Under Conditions of Risk.

Sharpe, W. F. (1964b). Capital Asset Prices: A Theory of Market Equilibrium Under Conditions of Risk.

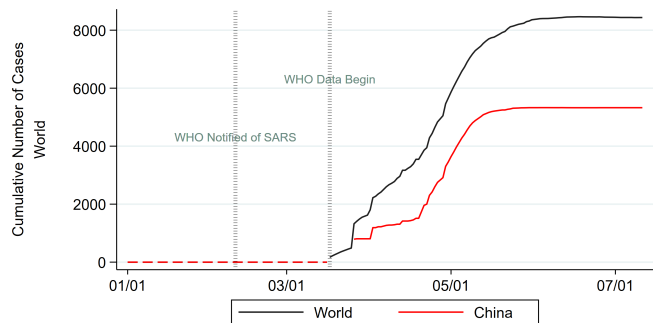
WHO (2006). *SARS: how a global epidemic was stopped*. Manila: WHO Regional Office for the Western Pacific.

Figure A.1: Actual COVID-19 Cases, By Country



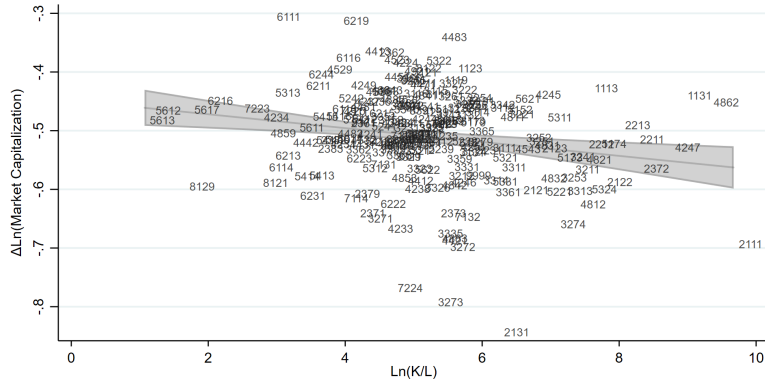
Source: Johns Hopkins Coronavirus Resource Center and authors' calculations. Figure displays the COVID-19 up to March 28.

Figure A.2: SARS Infections in China and Worldwide During 2003



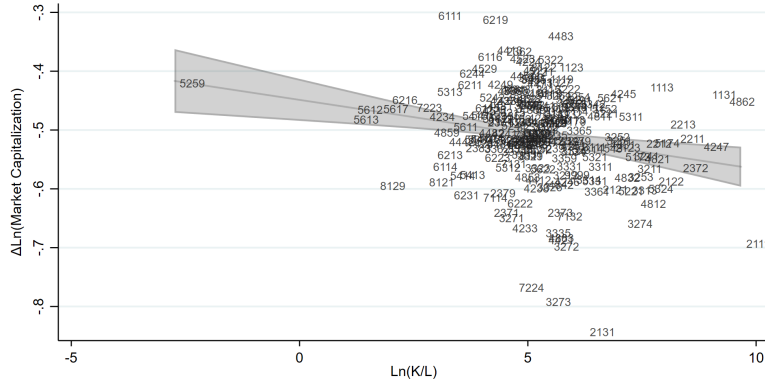
Source: World Health Organization and authors' calculations. Figure displays the cumulative reported SARS infections in China and the rest of the world from January 1, 2003 to July 11, 2003.

Figure A.3: Loss of Market Value and Initial Capital Intensity, by Industry



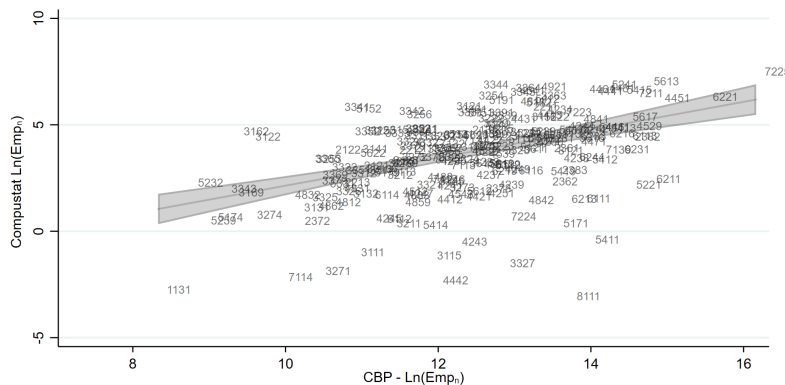
Source: Johns Hopkins Coronavirus Resource Center, Bloomberg, Yahoo Finance, Compustat and authors' calculations. Vertical axis is the cumulative change in market value from January 22 to April 10 due to COVID-19 across firms by four-digit NAICS industry, based on the coefficient in column 1 of Table 4. Horizontal axis is firms' fixed assets divided by their employment, also by four-digit NAICS sector.

Figure A.4: Loss of Market Value and Initial Capital Intensity (Unabridged)



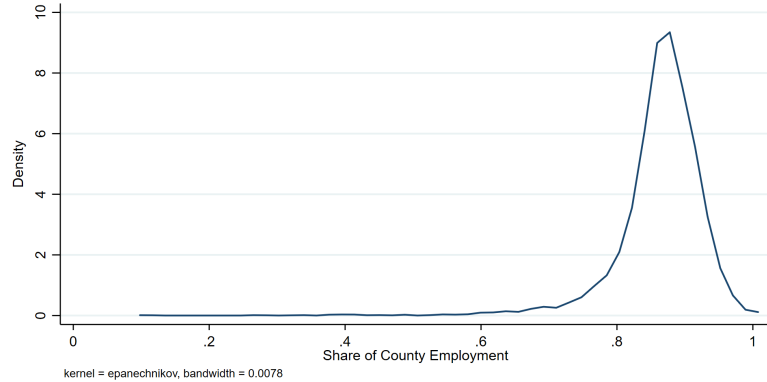
Source: Johns Hopkins Coronavirus Resource Center, Bloomberg, Yahoo Finance and authors' calculations. Figure reports the distribution of industry changes in market value implied by column 1 of Table 4 to industry capital to labor ratio.

Figure A.5: Employment in Compustat vs County Business Patterns



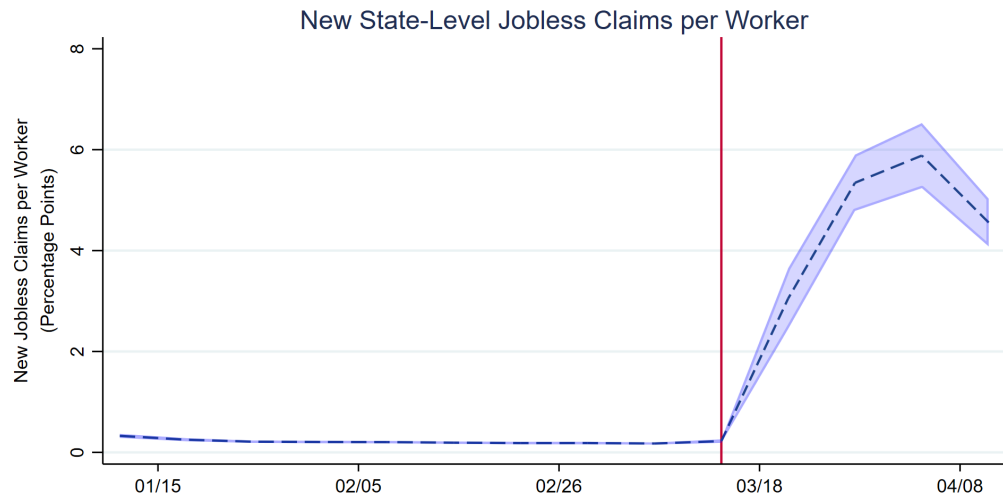
Source: Compustat, author's calculations, and County Business Patterns database.

Figure A.6: County Employment Coverage



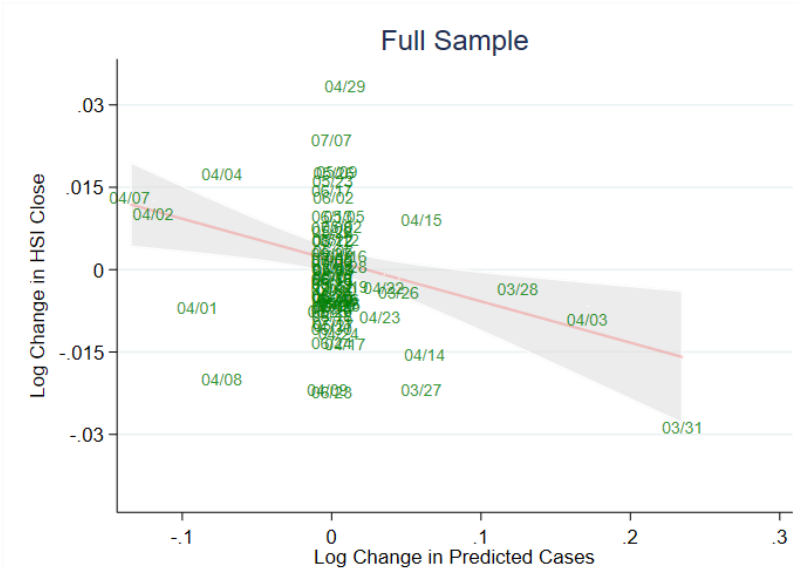
Source: Johns Hopkins Coronavirus Resource Center, Bloomberg, Yahoo Finance, County Business Patterns, Compustat, and authors' calculations. Figure reports the percent of county employment listed in CBP for which we have a matching naics-4 digit measure of $\Delta \ln(MV_n)$

Figure A.7: State Jobless Claims per Worker



Source: US Department of Labor. [Eckert et al. \(2020\)](#) and authors' calculations. Figure reports weekly initial jobless claims reported by the Department of Labor during 2020.

Figure A.8: Changes in Predicted SARS Cases vs HSI Index



Source: Johns Hopkins Coronavirus Resource Center, Yahoo Finance and authors' calculations. Figure displays the daily log change in the Hang Seng Index against the log change in projected cases for day t based on day $t - 1$ and day $t - 2$ information.